# Control over fine scale terrace structures induced on polycrystalline Pd by simple heat treatments in air

J.M. Sobral [a], T.W. Clyne [a], R. Rezk [b], A.E. Markaki [b],*

[a] Department of Materials Science and Metallurgy, Cambridge University, 27 Charles Babbage Road, Cambridge CB3 0FS, UK
[b] Department of Engineering, Cambridge University, Trumpington Street, Cambridge CB2 1PZ, UK

## ABSTRACT

This paper presents information about the formation of terraces (often composed of relatively wide faces and relatively narrow steps between them) on samples of polycrystalline palladium. These have been formed via simple heat treatments, involving holding at 1200 °C for periods ranging from a few minutes to several hours, followed by quenching by jets of inert gas. These treatments are such that the terraces are created, and survive the cooling, without significant formation of surface oxide. The crystallographic anisotropy of the surface energy is the driving force for terrace formation, with low surface energy planes tending to be preferentially exposed. Information is presented regarding the surface topography of the terraces and of the grain boundary regions, which have mainly been explored using AFM. Typically, the step heights are of the order of 50 nm and the widths of the faces between them are around 1 μm, although there are quite substantial local variations in these figures. It is shown that a degree of control is possible via the grain structure and texture of the sample, as well as via the processing conditions during the terracing treatment.

© 2017 The Authors. Published by Elsevier B.V. This is an open access article under the CC BY license (http://creativecommons.org/licenses/by/4.0/).

## 1. Introduction

In tissue engineering, physical cues such as topographical features, particularly in the nanometer scale, have been recognized as important for cellular function at the substrate/cell interface (see reviews [1,2]). In catalytic reactions, terraced nanomaterials have received a lot of attention over classical catalysts (see review [3]), which is highly related to their exposed crystallographic planes, as the atoms at different planes have different surface energy and surface charges.

It is well established that the surfaces of a range of material systems tend to reconstruct, by forming (fine scale) terrace structures, to minimize their surface energy even if this involves an increase in the total surface area (see recent review [4]). Such atomic scale reconstruction, predominantly in the form of surface diffusion, is driven by the crystallographic anisotropy of the surface energy. Spontaneous (large area) terracing can be achieved by heat treatment, requiring in some cases an ultra-high vacuum (UVH) environment. A typical terrace structure would contain a "face" which is expected to expose the lowest energy plane available. However, presumably it would not in general be possible for the entire grains to be composed entirely of these faces, since this would require a great deal of atomic movement, and for most grain orientations, this would lead to large inclinations between the surfaces of neighbouring grains and substantially greater overall surface area than if the whole sample were flat. Compromised terrace structures are

expected, incorporating periodic "steps" ("ledges"), also exposing crystallographic planes of relatively low energy, which allow the average inclination of the grain surface relative to the overall plane of the sample, and to neighbouring grains to be reduced.

Terrace structures have been mainly studied in single crystal systems, including metals (eg [5–12]), intermetallics (eg [13]), and oxides (eg [14–17]), but also in materials containing adsorbates on the surface (eg [18–23]). There are only a few experimental studies on terracing of polycrystalline surfaces [24–29], probably due to the increased complexity of multi-grained substrates, in which grain boundaries, as well as individual grain characteristics (such as crystallographic orientation and size), need to be taken into account. Nano-scale terraced surfaces have been observed [24–26] in 304 L austenitic (fcc) stainless steel after UHV heating at 1027 °C for 10–15 min. In these studies, using scanning tunnelling microscopy, the "faces" were interpreted as {111} planes, containing monatomic steps, 0.21 nm in height. The "steps" were deduced to be exposing {100} and {110} planes, which also have low surface energies. Terraced surfaces have also been observed [27] in polycrystalline 446 ferritic (bcc) stainless steel fibres after sintering at 1200 °C in a high vacuum system for a few hours. Using electron back-scattered diffraction and projection geometry, the crystallographic orientation of these terraces were found to correspond to low surface energy (low index) {110} and {211} crystallographic planes. However, the relatively sharp curvature of these fibres (~15 μm radius) complicates interpretation of these observations. Recently [28], sintered polycrystalline $UO_2$ was thermally etched to form terrace structures by annealing at 1500 °C for 1 h in an inert atmosphere. Using Synchrotron

Laue microdiffraction and scanning electron microscopy, terraces were found to expose one {100} plane and two {111} planes. Such observations have sometimes been interpreted in the light of theoretical studies on the expected anisotropy of the surface energy e.g. [30–37].

The creation of these terrace structures is highly dictated by the surface preparation techniques and experimental conditions. In general, the atmosphere, and hence the presence or absence of a surface oxide film is likely to affect the ease with which these terraces can form, since such a layer tends to inhibit surface diffusion of matrix atoms and reduces the crystallographic anisotropy of the surface energy. According to Ellingham Diagram data [38], which indicate the relative stability of metals with respect to their oxides, the oxides of "noble" metals (for example, gold (all temperatures) and silver (above ~200 °C)) are unstable and easily reduced. This makes them particularly attractive materials for studying terrace formation. On the other hand, the oxides of other metals are much harder to reduce. For example, stainless steels require extremely low oxygen partial pressures ($\approx 10^{-18}$ atm) to reduce the $Cr_2O_3$ oxide layer. Such oxygen pressures are difficult to achieve in conventional UHV systems. In the present study, a transition metal, palladium (Pd), was used to study terrace formation. Pd is more thermodynamically stable than its oxide PdO above ~900 °C, without the need for low oxygen partial pressures. Previous experimental study of terracing on Pd [11], which involved UHV heating a single crystal surface Pd(331) at 627 °C, generated a terraced surface exposing a mixture of {111}, {320} and {230} planes. Recently [29], a short study on terracing of planar polycrystalline Pd by the present authors aimed at describing the basic conditions under which polycrystalline palladium spontaneously reorganises by exposing terrace structures. The study examined how these structures change with heat treatment time. It was found that the step height and face width, within each terrace, and the grain size and grain boundary groove depth change with time tending to approach some sort of equilibrium. In the present study, an attempt is made to explain the resultant structures based on relevant characteristics of Pd (both crystallographic and thermodynamic), and the grain structure and texture of the samples. The angles between the planes of steps and adjacent faces are investigated as a function of heat treatment time. Guidelines for control of the resultant terrace structures are presented.

## 2. Experimental procedures

### 2.1. Material

Palladium rolled sheet of purity 99.95% (Goodfellow, UK) was used in this study. Discs, 8 mm in diameter and 0.5 mm in thickness, were cut from these sheets using a punch press.

### 2.2. Sample preparation

The discs were ground, using 1200 grit SiC paper, and then further polished with 6, 1 and 0.25 μm diamond paste, and finally 0.1 μm alumina suspension. They were cleaned sequentially with acetone, ethanol and finally isopropanol in an ultrasonic bath for 5 min each, with a final rinsing stage in ethanol, and then left to dry in air.

### 2.3. Heat treatment

The objective was to hold the samples at a temperature sufficiently high both to promote rapid diffusion and to ensure that oxide formation was not thermodynamically possible (above ~900 °C for Pd). In order to avoid extensive oxidation during cooling, this was carried out rapidly using gas quenching jets. All heat treatments were performed in a Carbolite MTF 12/25A 750 W tube furnace, equipped with a customized gas quenching system, which is shown schematically in Fig. 1. The cooling rates obtained using this quenching system were ~35 °C s$^{-1}$, so ambient temperature was reached in less than a minute. The palladium disks were placed in an alumina holder (SS52, Almath Crucibles Ltd., UK), heated at 1200 °C and quenched with gaseous nitrogen upon removal from the furnace.

### 2.4. Surface characterisation

#### 2.4.1. Scanning electron microscopy (SEM)

A JEOL 5800LV scanning electron microscope was used, in secondary electron imaging mode, to investigate the effects of annealing conditions and cooling rate, and also to monitor grain growth, step height and face width and grain boundary groove depth. An accelerating voltage of 10 kV and a working distance of approximately 10 mm were used.

#### 2.4.2. Atomic force microscopy (AFM)

Surface topography was investigated using a Digital Instruments Nanoscope v.7.30 (Veeco Instruments, UK) atomic force microscope, together with Scanning Probe Imaging Processor software (Image Metrology A/S, Denmark). The scanning frequency was adapted, depending on the scanned area and the type of surface, but in most cases it was between 0.3 and 0.5 Hz. All images were captured at a resolution of $512 \times 512$ pixels.
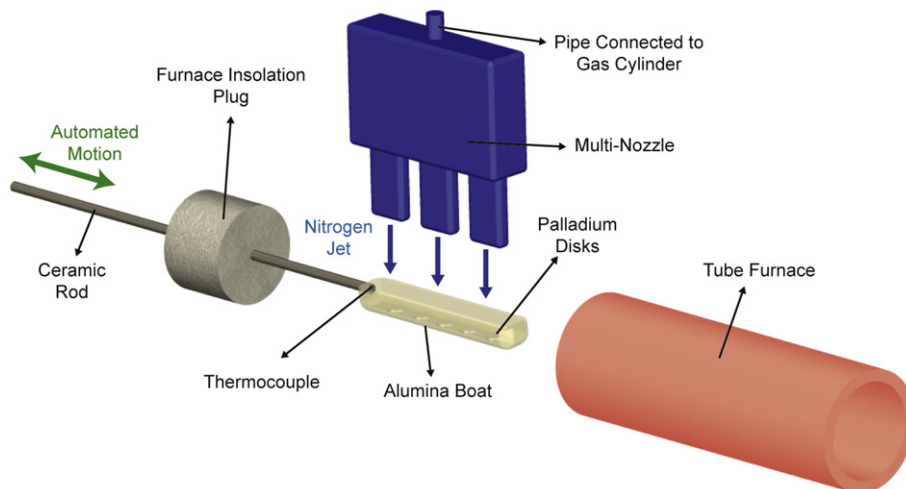


**Fig. 1.** Schematic of the automated setup used for heat treating the palladium discs, showing the gas quenching system.
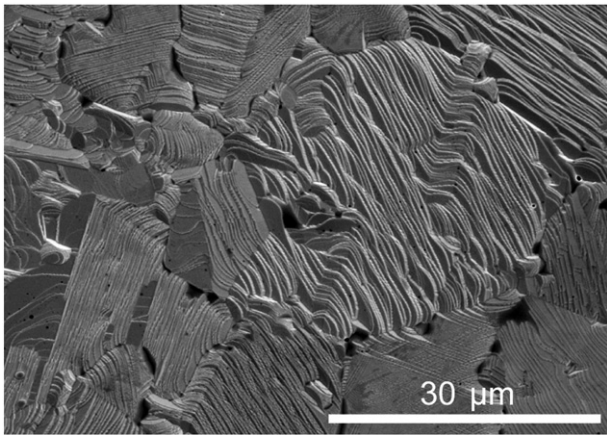
**Fig. 2.** SEM micrograph showing a polished Pd surfaces after heat treatment at 1200 °C for 30 min, followed by quenching in nitrogen.

## 3. Factors affecting terrace characteristics at room temperature

### 3.1. Basic effect

Fig. 2 shows an SEM micrograph of a Pd substrate after heating for 30 min at 1200 °C, followed by quenching with nitrogen jets. It can be seen that this treatment led to extensive terrace formation. This occurred in virtually all of the grains, although their orientation, and the spacing of the steps, varied substantially between them. Fig. 3 presents

3-D and 2-D AFM reconstructions of a typical terraced surface, together with line profiles taken within a terraced grain (blue line) and across a grain boundary (black line). It should, however, be noted that, while most terraces did appear to exhibit just two types of crystallographic plane, corresponding to "faces" and "steps", more complex surface structures are possible. For example, careful study of Fig. 2 reveals that, in some grains (e.g. the small one to the left of centre), the steps are themselves composed of two types of plane, while in others (e.g. the one at the bottom, to the right of centre) two sets of terraces are simultaneously present. Nevertheless, the predominant structure in most grains is a single terrace, with just two types of plane exposed.

Clarity is needed about the nomenclature being used, the relationship between measured parameters and the inherent characteristics of the surface being examined. This is shown in Fig. 4, in which this terminology is illustrated on a sectional sketch of a terrace and adjoining grain boundary, assuming that this section is oriented parallel to the maximum terrace gradient. The values of $\theta_1$ and $\theta_2$, shown in Fig. 4, will depend on the orientation of the grain concerned. Also, the angle between the planes of steps and adjacent faces $(\theta_2 - \theta_1)$ will be characteristic of the system assuming that the same two types of plane are being exposed in all cases, which may not be true. It should be noted that, in an AFM plot, the apparent value of this angle will differ from the true angle, unless the same scale is being used for vertical and horizontal measurements which would be unusual. For example, in Fig. 3, the terrace step height, $\Delta h$, is about 50 nm and the face width, $\Delta w$, is about 1000 nm, while the width of the step is about 200 nm. Applying some simple trigonometry, the angle $(\theta_2 - \theta_1)$ is about 160°, whereas it appears in Fig. 3 to be more like 120°. (The inclination of the terrace
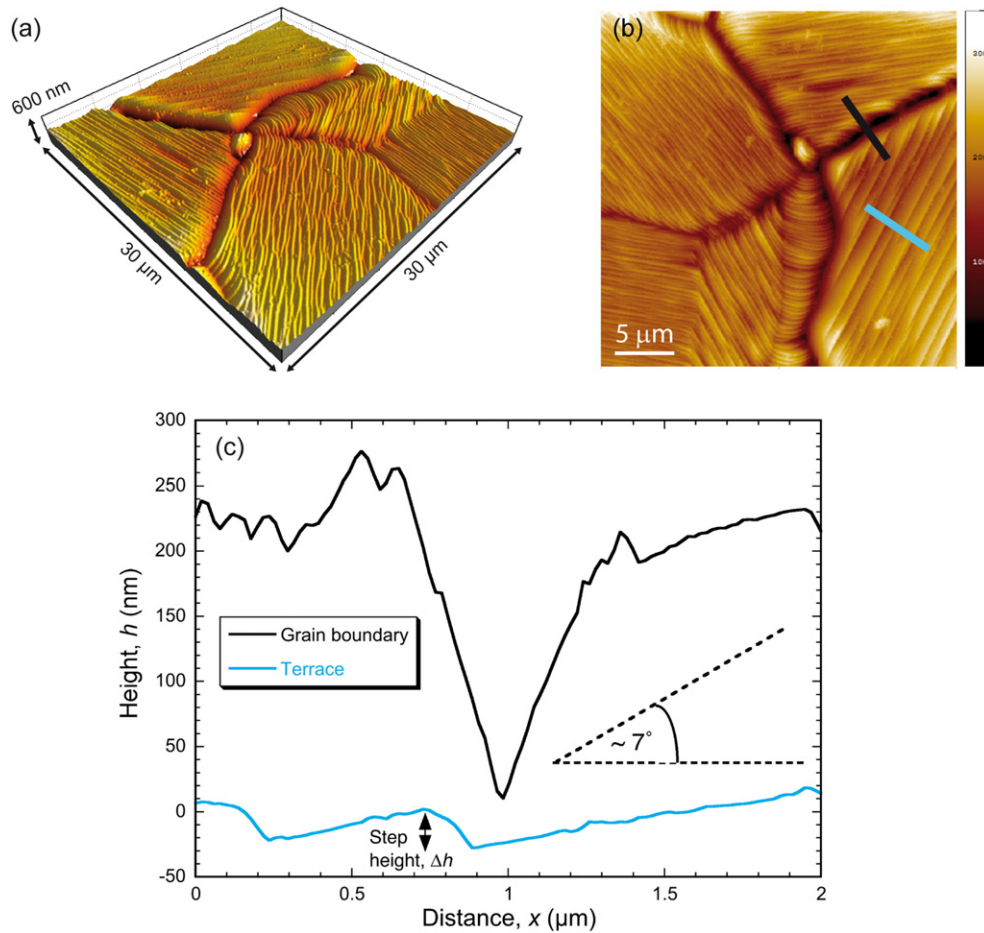






**Fig. 3.** (a) 3-D perspective and (b) 2-D plan view AFM reconstructions of the surfaces of polycrystalline polished samples after heat treatment at 1200 °C for 15 min, followed by gas quenching, and (c) line profiles across a grain boundary (black line in the 2-D view) and within a grain (blue line), showing the height and width of the terrace steps. (These profiles have been offset in height to avoid overlap.)
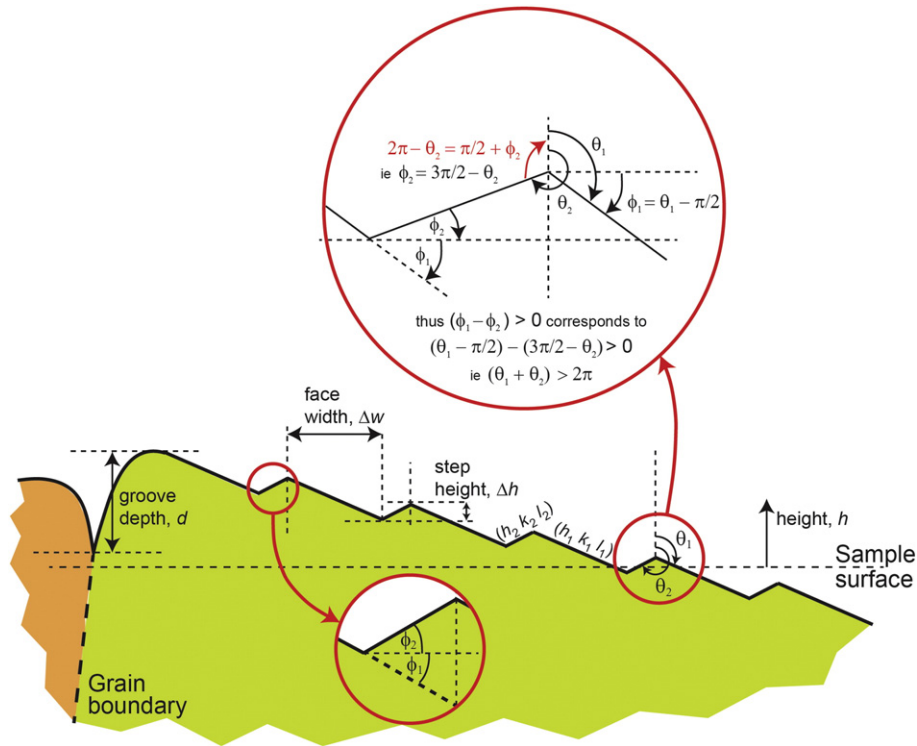
**Fig. 4.** Schematic depiction of a terrace near a grain boundary, showing the nomenclature being employed.

to the sample surface is thus somewhat exaggerated in Fig. 4.) It may also be noted that relatively deep grooves (~200 nm) can form at grain boundaries. There must, of course, be an energy penalty associated with these regions.

"Faces" form to minimize the total surface energy, even if this involves an increase in the total surface area. So this raises the question why the entire grain surface is not made up of such a face (single faceted grain) and whether periodic steps (ledges) are forming in order to reduce the overall area. The latter requires that $\phi_2$ is less than $\phi_1$ – see Fig. 4. From the expanded region in Fig. 4, simple trigonometry shows that this corresponds to $(\theta_2 + \theta_1) > 2\pi$, although the reduction would presumably need to be sufficient to compensate for the higher surface energy of the "step" face. Taking a typical value for $(\theta_2 - \theta_1)$ to be about $5\pi/6$ (see §3.5), this translates into a need for $\theta_1$ to be greater than about $7\pi/12$ – i.e. an inclination of the face to the sample surface of greater than about 15°, in order for the presence of steps to lead to a decrease in net surface area. In fact, most faces turn out to be less steeply inclined than this (see §3.5), so their role is presumably to allow the average angle of inclination of the grain surface to the sample surface to be reduced. Large inclinations of the grain surface would lead to grain boundary structures that carry substantial energy penalties because of the larger end-to-end height differences between neighbouring grains. Furthermore, there may have been insufficient diffusion time for the grain surface to reconstruct to form a single low energy face. To explore this, below we examine how the surface structures evolve with time.

### 3.2. Cooling conditions

As indicated in the Introduction, there is a driving force for oxidation of Pd below about 900 °C. It was observed that, if left to cool naturally in air from the heat treatment temperature, samples developed a purple sheen, indicating that a thick (at least of the order of the wavelength of light) surface oxide layer had formed. Little terracing was observable on such samples. This is illustrated by Fig. 5, which shows the microstructure of an air-cooled sample. It is, of course, likely that terraces did form at 1200 °C on this sample, in the same way as occurred with

the nitrogen-quenched sample shown in Fig. 2, but on the air-cooled one (Fig. 5) they have presumably become concealed by the formation of a thick oxide layer during the cooling process (between 900 °C and room temperature).

### 3.3. Grain growth

Grain growth during the heat treatment at 1200 °C is illustrated by the data in Fig. 6, which shows how the grain area of five non-neighbouring grains changed over a period of 12 h. Other grains in the vicinity must have been shrinking, but the selected grains all grew during this period. It can be seen that most of the grain growth took place during the initial 100–120 min.

### 3.4. Grain boundary groove depth

Changes in grain boundary groove depth during heat treatment at 1200 °C are shown in Fig. 7 for shorter and longer times. These were
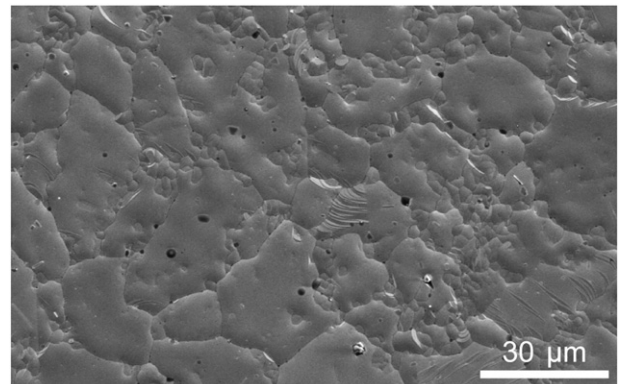


**Fig. 5.** SEM micrograph showing a polished Pd surface after prior annealing for 2 h at 600 °C and heat treatment at 1200 °C for 30 min, followed by natural cooling in air.
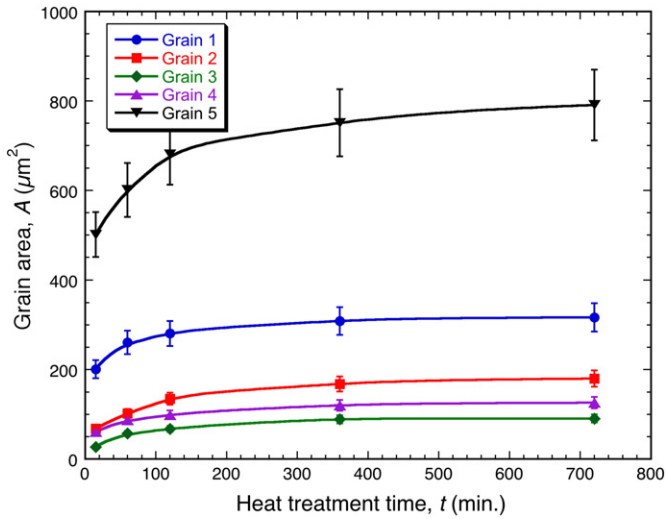
Fig. 6. Changes in measured areas of 5 selected grains in a sample, as a function of the (cumulative) duration of the heat treatment at 1200 °C.

obtained by averaging more than 30 AFM line profiles taken across six grain boundaries. It can be seen that, while the groove depths varied quite widely between different boundaries, they tended in all cases to increase with time, rising from initial values of ~100 nm to stabilized values ranging from 300 to 800 nm after periods of ~500 min. This

suggests that the groove depth at the grain boundaries tends to approach some form of equilibrium depending on the orientation relationship between the two neighbouring grains, and with the free surface, since these will dictate the inclination of the "faces" in the two grains. Presumably as the groove depth increases with heat treatment time, the faces would become more steeply inclined to the sample surface. However, it should be recognized that the surface as a whole cannot closely approach true equilibrium, not without the sample becoming a single crystal - and, as with any bulk grain growth process (ignoring these surface-related effects of terrace and groove formation), any particular locality cannot adapt in complete isolation of neighbouring regions. For example, individual grains often grow initially, but then shrink and perhaps disappear. Effects of this type are apparent in Fig. 8, which shows AFM reconstructions of a region after periods of 120, 360 and 720 min at 1200 °C.

### 3.5. Step height and face width

Changes in grain size and grain boundary groove depth are accompanied by changes in height of the individual steps and the width of the faces between them, within each terrace. This is shown in Fig. 9. The data suggest that a "stable" step height and face width is achieved relatively quickly for most of the grains. This may be attributed to the fact that it involves surface diffusion over shorter distances than that needed for grain growth. However it should be emphasized, the full picture is again more complex than this, since the average inclination of the surface of a grain and the grain size may be changing, so the most stable
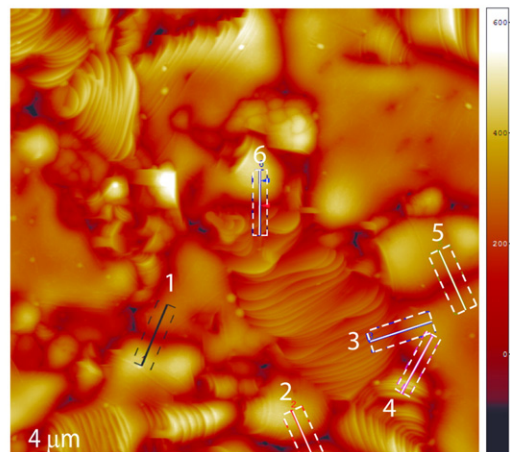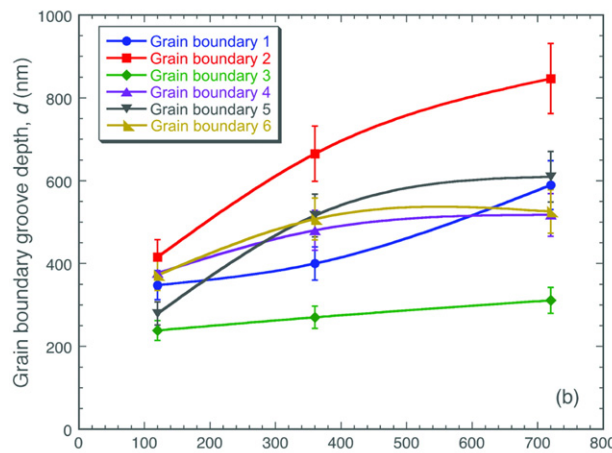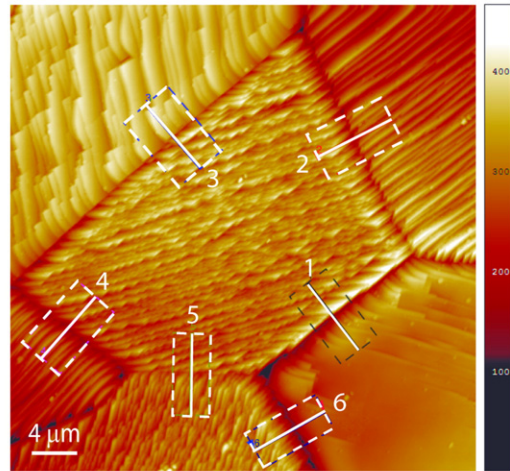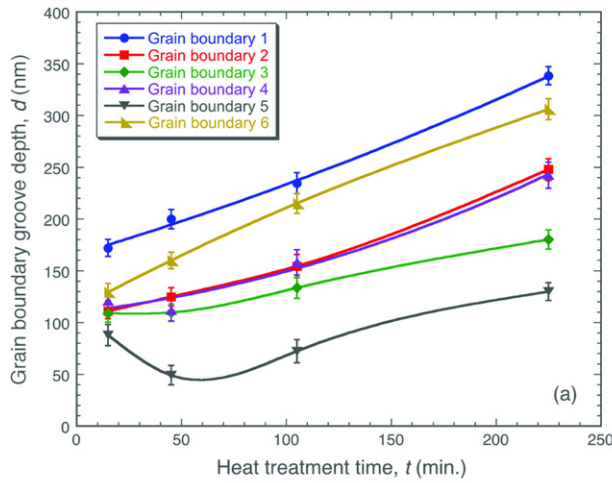


Fig. 7. Changes in the measured depth of the grooves in particular sets of grain boundaries, as a function of the (cumulative) duration of the heat treatment at 1200 °C, for two samples, exposed to (a) short and (b) longer periods at this temperature. AFM 2-D visualisations for the particular sets of grain boundaries are also shown.
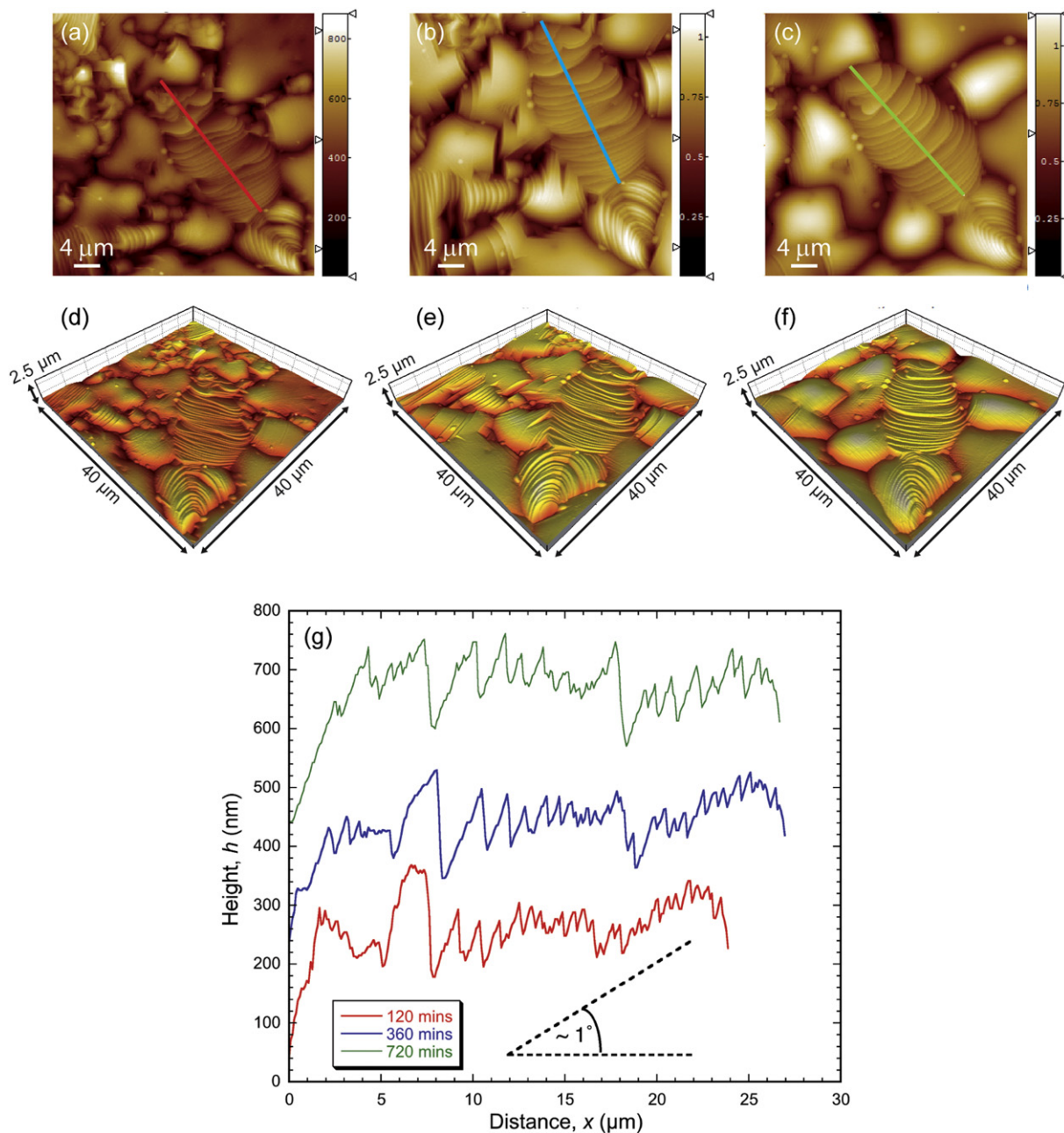
**Fig. 8.** AFM 2-D (a–c) and 3–D (d–f) visualisations for a sample after heat treatment times at 1200 °C of (a), (d) 120, (b), (e) 360 and (c), (f) 720 min, showing the lines along which the profiles are plotted in (g), with arbitrary vertical offsets to separate the three plots.

ratio of step area to face area for a particular grain may change with time. This is reflected in the data in Fig. 9, where it can be seen that slightly different trends are observed in different grains.

Fig. 10 shows the measured angle between the planes of steps and adjacent faces as a function of heat treatment time. Measurements were taken from six selected grains in different samples. The angles were found to be about 140–160° in all cases, suggesting that, at least in most cases, they are all the same types of crystallographic plane. It's likely that these are {111} and {110} planes, which are expected to be low energy planes in fcc crystals and are inclined at about this angle. Since {111} planes are expected to exhibit the lowest surface energy (because they are close-packed), these will be the "faces" – i.e. the planes that tend to predominate, while the "steps" allow the average inclination of the grain surface to remain fairly close to the plane of the overall sample surface and are probably {110} planes. It follows that the spacing of the steps is likely to depend on the grain orientation.

This effect is apparent in Fig. 9 and Fig. 11. Fig. 11 shows how the topography changes with treatment time in two different grains. It can be seen that in grains with a {111} plane fairly close to the sample surface, such as that in Fig. 11(a), the steps tend to disappear, while in others (the majority), such as Fig. 11(b), their presence is required to ensure that the average angle of inclination of the grain surface relative to the sample surface remains low.

### 3.6. Prediction and control of terrace structure

In summary, it's clear that extensive terracing is readily produced on (polycrystalline) Pd. This is dependent on its oxidation characteristics and the crystallographic anisotropy of its surface energy, both of which appear to be well-suited for the creation of terraces. Since the processing is easy and relatively simple, and Pd is appreciably cheaper than Au (but not Ag), this may be of potential commercial
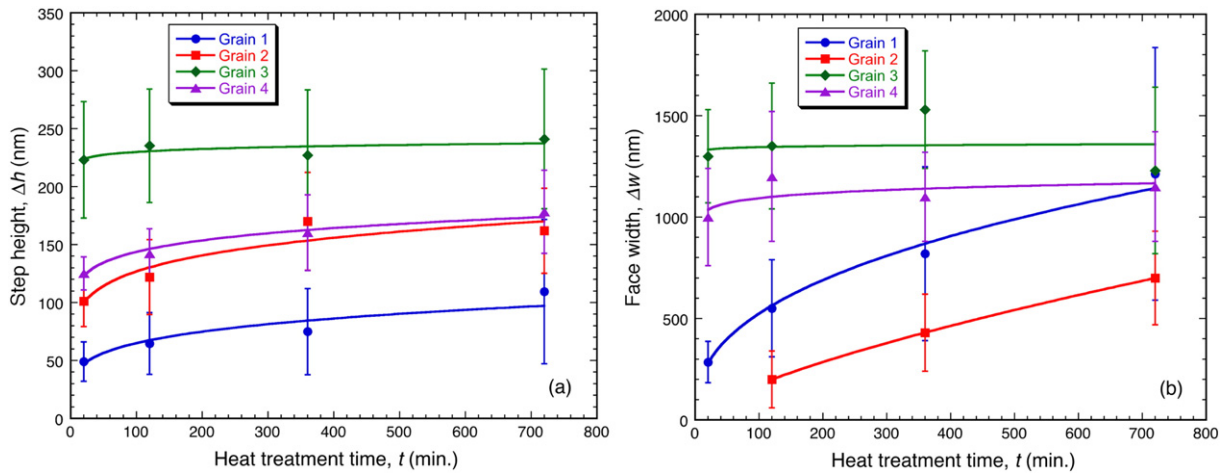
**Fig. 9.** AFM data showing, as a function of heat treatment time at 1200 °C, the average values of (a) step height and (b) face width within 4 different grains in a sample.

interest. Of course, it would be possible to create Pd coatings on a range of substrates, and it's expected that these would form terraces in a similar way (while protecting the substrate from oxidation).

It's also clear that a degree of control can be exercised over the terrace structure. Longer heat treatments (and presumably higher temperatures) in general lead to coarser structures with larger step heights. However, the terrace structure will largely depend on the local grain–grain correlations of the crystallographic orientation. As illustrated in Fig. 11, the surface structure tends to approach some sort of equilibrium, in which steps are retained – i.e. the individual grain surfaces do not all become single faces of the lowest surface energy plane. If the atoms on the surface would reconstruct to the extent that the exposed surface is entirely composed of a single-faceted plane, that would create terrace surfaces quite steeply inclined to the sample surface, leading to large exposed areas at the grain boundaries. This suggests that there is an energy barrier to the complete removal of steps and it's probable that this is associated with the grain boundary structures.

No systematic measurements have been made of the crystallographic orientations of exposed faces, but it seems likely that at least many of them are {111} planes, which are expected in fcc structures to exhibit the lowest surface energy. The angle between steps and faces has been consistently measured to be about 140–160°, which is broadly equal to the expected angle between appropriate

{111} and {110} planes (~145°). However, it should be noted that the maximum inclination between a sample surface and the nearest {111} plane normal is about 54° (for a {100} surface). It was rare to see faces that appeared to be inclined to the sample surface at any angles remotely approaching this range. On the other hand, it was also rare to see grains that did not exhibit terraces. It follows that there were almost certainly at least some cases in which planes other than {111} formed the faces. It must, however, be recognized that texture plays a potentially important role. The rolled sheet used in this work was almost certainly heavily textured and this texture may, for example, have been such that there were no {100} planes oriented close to the free surface.

It follows from the above points that a degree of control is possible (via the grain structure and texture of the sample, as well as via the processing conditions during the terracing treatment), although there are several complex interacting effects at play and in general it is likely that experimentation will be needed to optimize the final structure for specific purposes.

## 4. Conclusions

(a) It's been shown that, by carrying out heat treatments at 1200 °C, followed by quenching to room temperature in jets of nitrogen, a variety of terrace structures can be created on the surface of polycrystalline palladium samples. This occurs by surface diffusion, which creates structures with lower free energy (influenced by the crystallographic anisotropy of the surface energy), with the quenching in inert gas needed to avoid significant oxide formation as the material comes into the temperature range (below about 900 °C) where this is thermodynamically favoured.

(b) The terrace structures tend to become coarser as the heat treatment time is extended, although, for any given grain, the average inclination angle of the grain surface relative to the overall plane of the sample tends to remain fairly constant with extended treatment and in general does not exceed a few degrees.

(c) The crystallographic faces being exposed are thought to be predominantly {111} planes, and the steps are probably {110} planes. The angles between steps and faces were measured to be around 150° in the majority of cases, changing little with extended heat treatment time. This is consistent with the proposed types of plane. It should, however, be recognized that the details of the structure depend on the orientation relationships between neighbouring grains, and on the overall texture of the sample.
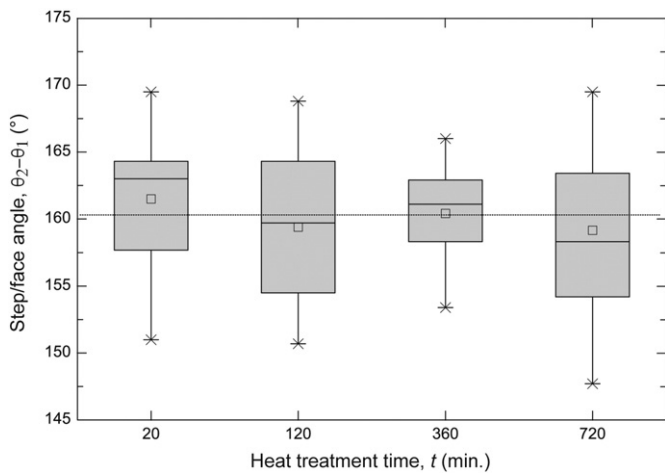


**Fig. 10.** Measured angle between the planes of steps and adjacent faces of terraces in 6 selected grains (from different samples), as a function of heat treatment times at 1200 °C. The values represent minimum, 25th percentile, mean, median, 75th percentile and maximum magnitudes.
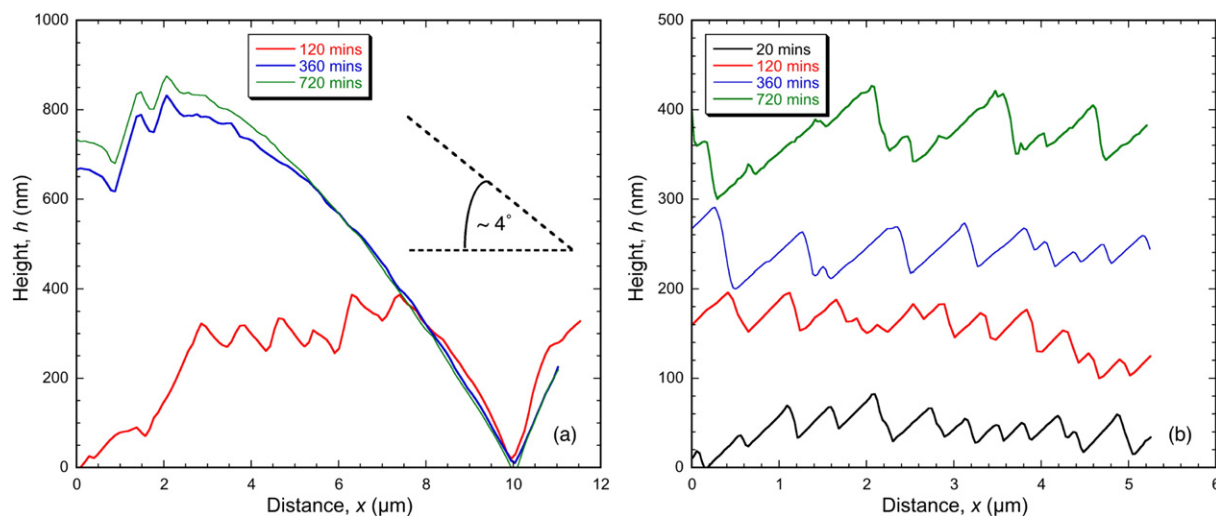
**Fig. 11.** AFM data showing profiles across two different grains, after different heat treatment times at 1200 °C, for (a) a grain in which the steps largely disappear and (b) one in which they persist (with the profiles offset to avoid overlap).

(d) Deep grooves tend to form at grain boundaries, particularly if there is a relatively large angle between the average inclinations of the surfaces of the two grains concerned. It's thought that the energy associated with the grain boundary regions may be at least partly responsible for the average inclination angles of individual grains, relative to the sample surface, having a tendency to remain relatively low. The presence of the steps assists this, and so in most cases they tend to persist over long treatment times.

## References

[1] M. Nikkhah, F. Edalat, S. Manoucheri, A. Khademhosseini, Engineering micro-scale topographies to control the cell-substrate interface, Biomaterials 33 (2012) 5230–5246.
[2] A.T. Nguyen, S.R. Sathe, E.K.F. Yim, From nano to micro: topographical scale and its impact on cell adhesion, morphology and contact guidance, J. Phys. Condens. Matter 28 (2016).
[3] J. Pal, T. Pal, Faceted metal and metal oxide nanoparticles: design, fabrication and catalysis, Nano 7 (2015) 14159–14190.
[4] D.P. Woodruff, Adsorption and reaction at stepped surfaces: a historical viewpoint, J. Phys. Condens. Matter 28 (2016).
[5] R. Bryl, T. Olewicz, T.V. de Bocarme, N. Kruse, Thermal faceting of clean and oxygen-covered Ir nanocrystals, J. Phys. Chem. C 115 (2011) 2761–2768.
[6] H. Xie, H.W. Zhang, J.G. Li, K. Lu, Local faceting in coarsening of nanolaminates with low angle boundaries in pure nickel, Scr. Mater. 122 (2016) 110–114.
[7] A.V. Butashin, V.P. Vlasov, V.M. Kanevskii, A.E. Muslimov, V.A. Fedorov, Specific features of the formation of terrace-step nanostructures on the (0001) surface of sapphire crystals, Crystallogr. Rep. 57 (2012) 824–830.
[8] L. Guillemot, K. Bobrov, Morphological instability of the Cu(110)-(2 × 1)-O surface under thermal annealing, Phys. Rev. B 83 (2011), 075409.
[9] K.M. McElhinny, R.M. Jacobberger, A.J. Zaug, M.S. Arnold, P.G. Evans, Graphene-induced Ge (001) surface faceting, Surf. Sci. 647 (2016) 90–95.
[10] M. El-Jawad, B. Gilles, F. Maillard, Oxygen-induced formation of nanopyramids on W(111), in: M. Soueidan, M. Roumie, P. Masri (Eds.),Advances in Innovative Materials and Applications 2011, pp. 109–112.
[11] P.W. Davies, R.M. Lambert, Structural stability and chemisorption properties of a stepped palladium surface: O₂ and NO on Pd(331), Surf. Sci. 110 (1981) 227–249.
[12] F. Silva, A. Martins, Surface reconstruction of gold single crystals: electrochemical evidence of the effect of adsorbed anions and influence of steps and terraces, Electrochim. Acta 44 (1998) 919–929.
[13] G.M. McGuirk, J. Ledieu, E. Gaudry, M.C. de Weerd, M. Hahne, P. Gille, D.C.A. Ivarsson, M. Armbruster, J. Ardini, G. Held, F. Maccherozzi, A. Bayer, M. Lowe, K. Pussi, R.D. Diehl, V. Fournee, The atomic structure of low-index surfaces of the intermetallic compound InPd, J. Chem. Phys. 143 (2015), 074705.
[14] O. Bierwagen, J. Rombach, J.S. Speck, Faceting control by the stoichiometry influence on the surface free energy of low-index bcc-In2O3 surfaces, J. Phys. Condens. Matter 28 (2016) 224006.
[15] G.S. Parkinson, P. Lackner, O. Gamba, S. Maass, S. Gerhold, M. Riva, R. Bliem, U. Diebold, M. Schmid, Fe3O4(110)-(1 × 3) revisited: periodic (111) nanofacets, Surf. Sci. 649 (2016) 120–123.
[16] R. Verre, R.G.S. Sofin, V. Usov, K. Fleischer, D. Fox, G. Behan, H. Zhang, I.V. Shvets, Equilibrium faceting formation in vicinal Al2O3 (0001) surface caused by annealing, Surf. Sci. 606 (2012) 1815–1820.
[17] Y. Wang, S. Lee, P. Vilmercati, H.N. Lee, H.H. Weitering, P.C. Snijders, Atomically flat reconstructed rutile TiO2(001) surfaces for oxide film growth, Appl. Phys. Lett. 108 (2016), 091604.
[18] Q. Chen, N.V. Richardson, Surface facetting induced by adsorbates, Prog. Surf. Sci. 73 (2003) 59–77.
[19] P. Kaghazchi, D. Fantauzzi, J. Anton, T. Jacob, Nanoscale-faceting of metal surfaces induced by adsorbates, Phys. Chem. Chem. Phys. 12 (2010) 8669–8684.
[20] P. Kaghazchi, T. Jacob, I. Ermanoski, W.H. Chen, T.E. Madey, New surfaces stabilized by adsorbate-induced faceting, J. Phys. Condens. Matter 24 (2012) 265003.
[21] T.E. Madey, W. Chen, H. Wang, P. Kaghazchi, T. Jacob, Nanoscale surface chemistry over faceted substrates: structure, reactivity and nanotemplates, Chem. Soc. Rev. 37 (2008) 2310–2327.
[22] I.S. Rakic, M. Kralj, W. Jolie, P. Lazic, W.H. Sun, J. Avila, M.C. Asensio, F. Craes, V.M. Trontl, C. Busse, P. Pervan, Step-induced faceting and related electronic effects for graphene on Ir(332), Carbon 110 (2016) 267–277.
[23] S. Schmitt, A. Scholl, E. Umbach, Long-range surface faceting induced by chemisorption of PTCDA on stepped Ag(111) surfaces, Surf. Sci. 643 (2016) 59–64.
[24] A. Stupnik, M. Leisch, Atom probe and STM study on stainless steel after vacuum firing, Vacuum 82 (2007) 170–173.
[25] A. Stupnik, M. Leisch, Study on the surface topology of vacuum-fired stainless steel by scanning tunnelling microscopy, Vacuum 81 (2007) 748–751.
[26] A. Stupnik, P. Frank, M. Leisch, Atom probe, AFM, and STM studies on vacuum-fired stainless steels, Ultramicroscopy 109 (2009) 563–567.
[27] A.E. Markaki, K.M. Knowles, R.A. Oliver, A. Gholinia, Surface terracing on ferritic stainless-steel fibres and potential relevance to in vitro cell growth, Philos. Mag. 89 (2009) 2285–2303.
[28] Y.B. Miao, K. Mo, T.K. Yao, J. Lian, J. Fortner, L. Jamison, R.Q. Xu, A.M. Yacout, Correlation between crystallographic orientation and surface faceting in UO2, J. Nucl. Mater. 478 (2016) 176–184.
[29] J.M. Sobral, T.W. Clyne, R. Rezk, A.E. Markaki, Nano-terracing on polycrystalline palladium induced via simple heat treatment, Scr. Mater. 130 (2017) 17–21.
[30] C. Herring, Some theorems on the free energies of crystal surfaces, Phys. Rev. 82 (1951) 87–93.
[31] M. Methfessel, D. Hennig, M. Scheffler, Trends of the surface relaxations, surface energies, and work-functions of the 4d transition-metals, Phys. Rev. B 46 (1992) 4816–4829.
[32] L. Vitos, A.V. Ruban, H.L. Skriver, J. Kollar, The surface energy of metals, Surf. Sci. 411 (1998) 186–202.
[33] J.M. Zhang, F. Ma, K.W. Xu, Calculation of the surface energy of FCC metals with modified embedded-atom method, Appl. Surf. Sci. 229 (2004) 34–42.

[34] L.H. Duan, L.H. Pan, Q. Li, X.H. Meng, Q. Wang, X.L. Zhuang, M.L. Ling, L.J. Song, Density functional theory studies of the palladium-silver(211) stepped surfaces, J. Nanosci. Nanotechnol. 14 (2014) 7079–7086.

[35] M. Jo, Y.W. Choi, Y.M. Koo, S.K. Kwona, Scaling behavior of the surface energy in face-centered cubic metals, Comput. Mater. Sci. 92 (2014) 166–171.

[36] J. Wang, S.Q. Wang, Surface energy and work function of fcc and bcc crystals: density functional study, Surf. Sci. 630 (2014) 216–224.

[37] B. Wang, J.M. Zhang, Y.D. Lu, X.Y. Gan, B.X. Yin, K.W. Xu, Anisotropy analysis of surface energy and prediction of surface segregation for fcc metals, Acta Phys. Sin. 60 (2011), 016601.

[38] H.J.T. Ellingham, Reducibility of oxides and sulfides in metallurgical processes, J. Soc. Chem. Ind. Lond. 63 (1944) 125–133.